

# Cross-link in norbornadiene-based polymers from ring-opening metathesis polymerization with pyrrolidine-based Ru complex

Larissa R. Fonseca<sup>1</sup> · José L. Silva Sá<sup>2</sup> · Valdemiro P. Carvalho Jr.<sup>3</sup> · Benedito S. Lima-Neto<sup>1</sup>

Received: 31 July 2017 / Revised: 5 November 2017 / Accepted: 13 November 2017 /

Published online: 18 November 2017

© Springer-Verlag GmbH Germany, part of Springer Nature 2017

**Abstract** Ring-opening metathesis polymerization (ROMP) of norbornadiene (NBD) with  $[\text{RuCl}_2(\text{PPh}_3)_2(\text{pyrrolidine})]$  as the starting complex was evaluated as a function of reaction time, solvent volume, and atmosphere type at 25 °C. Quantitative yields of polyNBD were obtained either under inert argon atmosphere or in air, with 2 mL of  $\text{CHCl}_3$ , for 30 min. Copolymerization of NBD with norbornene (NBE) resulted in 100–70% yield under argon, depending on the NBE/NBD molar ratio, and in 70% yield in air, with 2 mL, for 120 min. TGA, DSC, and DMA measurements and swelling tests supported the occurrence of cross-linking in homopolyNBD and in the copolymers isolated from polymers. SEM micrographs showed porous polymeric NBD materials with pores that decreased in size when increasing the amount of NBD in the starting reaction composition. Results from amine parent complexes when the amine was piperidine or perhydroazepine are also discussed, with high cross-linking degree from reaction with the pyrrolidine complex.

**Keywords** ROMP · Norbornene · Norbornadiene · Ruthenium · Ancillary ligand · Non-carbene complexes

**Electronic supplementary material** The online version of this article (<https://doi.org/10.1007/s00289-017-2236-3>) contains supplementary material, which is available to authorized users.

✉ Benedito S. Lima-Neto  
benedito@iqsc.usp.br

<sup>1</sup> Instituto de Química de São Carlos, Universidade de São Paulo, CP 780, São Carlos, SP CEP 13560-970, Brazil

<sup>2</sup> Centro de Ciências da Natureza, Universidade Estadual do Piauí, Teresina, PI CEP 64002-150, Brazil

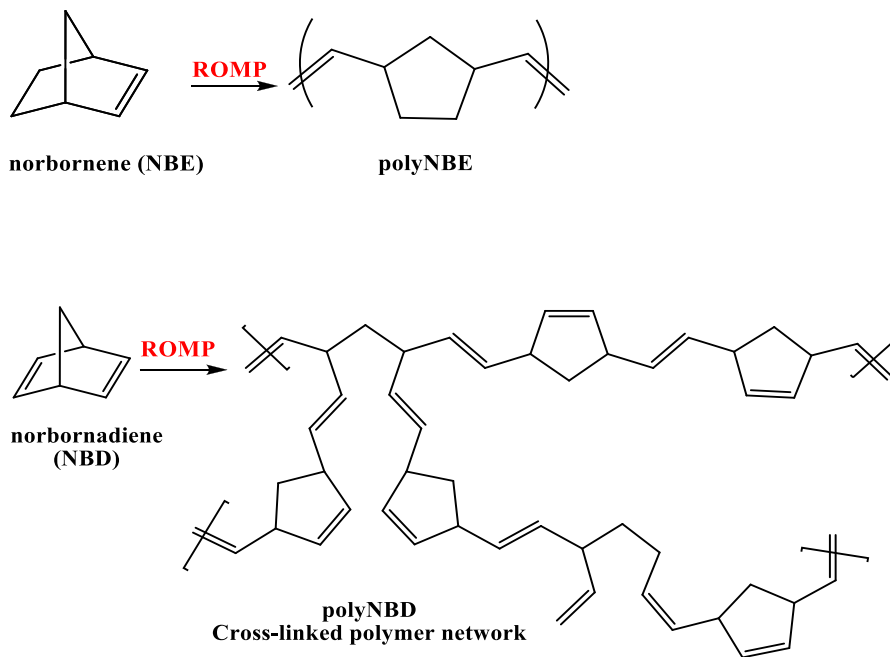
<sup>3</sup> Faculdade de Ciências e Tecnologia, UNESP Univ Estadual Paulista, Presidente Prudente, SP CEP 19060-900, Brazil

## Introduction

Ring-opening metathesis polymerization (ROMP) of cyclic olefin has been an efficient method to develop polymers and copolymers for practical applications in different fields of science, including functionalized polymeric materials with advanced structures [1–7]. Pendant functional groups in the cyclic olefin, such as carboxylic or hydroxyl, are useful to be modified into many other groups for the development of unlike polymers [8, 9].

ROMP is a typical coordination polymerization, but the ring strain in the cyclic olefin is important for the reaction to occur; the energy released upon the ring opening contributes to the reaction driving force [10–13]. Norbornene (NBE), with a strain cycle of  $27.2 \text{ kcal mol}^{-1}$  [14], can easily undergo ROMP (Scheme 1), and it is usually employed in tuning catalytic activity.

Polyolefins obtained via ROMP from strained cyclic olefins are usually stereoregular, monodisperse, and present high molecular weight; they are also an important commercial class of synthetic thermoplastics [6]. PolyNBE is amorphous thermoplastic with molecule chains chaotically arranged. As expected, thermoplastics are materials that become soft when heated and hard when cooled; however, the presence of a cross-linking agent, such as norbornadiene (NBD), can change their properties, such as brittleness, thermal stability, morphology, and others [15]. Therefore, NBD also presents large chemical interest because the opening of the second ring forms a cross-linked polymeric structure (Scheme 1). This second



**Scheme 1** Illustration of ROMP of NBE and NBD

opening is thermodynamically less favourable than the first double ring, and very often a double coordination bond occurs, poisoning the starting metal complex or the catalyst species in the propagation reaction [16, 17]. In this way, to avoid this fact, selection of the metal-ancillary ligand dual pair to catalyse ROMP implies in the success of the resulting polymer, whose identity can range from a cross-linked and insoluble polymer to one that is linear and usually soluble in regular solvents.

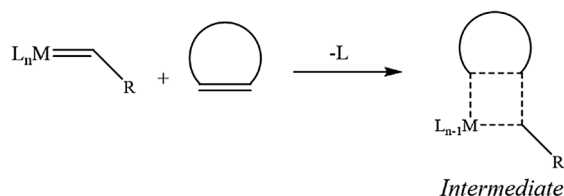
A transition metal carbene complex catalyses ROMP via a metallocyclobutane intermediate formed from the interaction between a metal carbene moiety and the cyclic olefin, resulting in rearrangement of the carbon–carbon double bond [18–21], as illustrated in Scheme 2 [6].

Currently, many metal carbene complexes are well established, in which a diversity of ancillary ligands provide electronic and geometric arrangements for occurrence of the metal–olefin bonding and subsequent formation of the metallocyclobutane intermediate. An important key in this process is the orbital coplanarity between the metal carbene moiety and the olefin, as well as prevention of double coordination in the case of polycyclic multiple olefins. Therefore, the search for ancillary ligands to support these features is a continuous target.

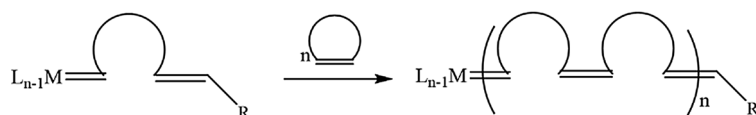
Commercially available Grubbs-type catalysts are the most commonly used initiators for ROMP reactions in both academia and industry [6]. An alternative to these catalysts is the development of highly active and robust compounds that can be easily prepared at low production cost. In particular, our group has been working extensively on the development of catalysts to mediate reactions with high molar ratios of [monomer] to [Ru] for few minutes at room temperature [17, 22–30].

In particular, our research group has been studying ROMP with well-defined non-carbene  $[\text{RuCl}_2(\text{PPh}_3)_2(\text{amine})]$  complexes; the catalytic species is produced in situ from reaction with ethyl diazoacetate (EDA) [17, 22–30]. Some advantages of these types of complexes are associated with the conditions of synthesis, storage, and manipulation. These circumstances corroborate the literature, which has claimed application of metathesis in more user-friendly conditions [31] considering the

### Initiation



### Propagation



**Scheme 2** Illustration of ROMP catalysed by a transition metal carbene complex

entire process: from the synthesis of the catalyst to its application in olefin metathesis. So far, our results have presented satisfactory reactivity, forming polymers and copolymers in high yields, with different thermal and morphological characteristics [26, 28].

ROMP of NBE under argon atmosphere and in non-degassed solvent (in air) at room temperature using the  $[\text{RuCl}_2(\text{PPh}_3)_2(\text{amine})]$  complex type has been successfully conducted with the amines pyrrolidine (complex **1**), piperidine (complex **2**), and perhydroazepine (complex **3**) as ancillary ligands (Fig. 1) [17, 22]. Different reactivity, yields, and polymer characteristics have been observed with the complexes **1**, **2**, and **3**. A propagating species without  $\text{PPh}_3$  ligands in the metal coordination sphere has been demonstrated by calculus in the case with **2** [32]. Thus, the different amine ring size drives the reaction, considering that the cyclic amines present rings which differ by one  $\text{CH}_2$  unit (Fig. 1) and that the amines must present similar  $\sigma$ -donor nature [17, 22, 27, 29].

With complex **1**, the ratios of yields for ROMP of NBE from the runs under argon atmosphere and in air were close to the unit, indicating an insignificant loss of reactivity of the active species in the presence of  $\text{O}_2$  from air. Studies with NBD and copolymers with NBE were not investigated. Therefore, the purpose of this study is to investigate ROMP of NBD and its copolymerization with NBE using complex **1** to compare the results with those obtained with the complexes **2** and **3** [17, 27]. It is expected that the present study provide further support to discuss ring size influence on cyclic amines as ancillary ligands in Ru–amine-based complexes for ROMP of bicyclic monomers. This would improve knowledge about the properties of the obtained polymers utilizing these parent complexes as catalytic initiators in an interface of the development joining catalyst and polymer sciences. As concluded, shifts in the thermoplastic nature and microstructure of the polymers were obtained. An important fact is the type of resulting polymer from usual monomers, tailored by simple complexes.

Experiments are performed under argon atmosphere and in air to observe the stability of the active metal species in the presence of molecular oxygen from air. Experiments are performed with different volumes of solvent to observe entropic effects. All reactions are followed as a function of time.

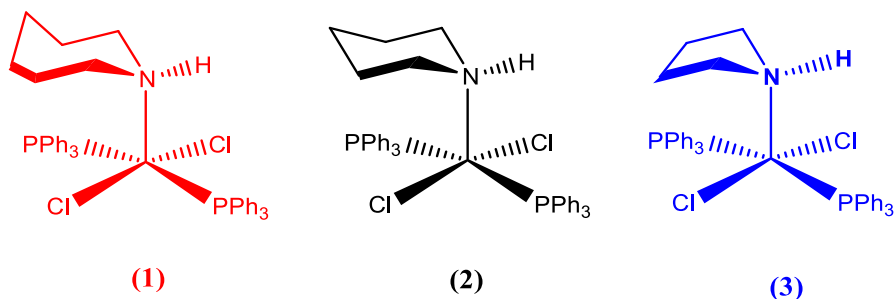


**Fig. 1** Illustration of the Ru–amine complexes with pyrrolidine (**1**), piperidine (**2**), and perhydroazepine (**3**)

## Experimental

### General remarks

Norbornene (NBE), norbornadiene (NBD), and ethyl diazoacetate (EDA) from Aldrich were used as obtained. Other commercially available reagents were used without further purification. All the solvents were of analytical grade. The  $[\text{RuCl}_2(\text{PPh}_3)_2(\text{amine})]$  complexes, with pyrrolidine (**1**), piperidine (**2**), and perhydroazepine (**3**) were obtained following the literature [17, 22, 29].

### Polymerization

In a typical ROMP experiment, NBD was dissolved in  $\text{CHCl}_3$ . In the case of the copolymerization reactions, NBD and NBE were dissolved in the same flask. The Ru–amine-based complex (1.0 mg) was added to the reaction solution, followed by 5.0  $\mu\text{L}$  of EDA. The molar ratio  $[\text{monomer}]/[\text{Ru}]$  was 5000. Mixtures of monomers (NBE with NBD) were prepared using different NBD loadings, ranging from 20 to 80%, and NBE as balance. Polymerization was performed at  $23 \pm 1^\circ\text{C}$  in silicone oil bath. The reactions were performed under argon (in degassed  $\text{CHCl}_3$ ) or under air (in non-degassed  $\text{CHCl}_3$ ) to evaluate the reactivity of the complex. After the desired reaction time, 20 mL of methanol was added and the precipitated polymer was filtered, washed with methanol, and dried in vacuum before being weighed. The yields reported are the arithmetic averages from a batch with two individual solutions, and each batch was performed at least three times up to an experimental error of 5–10%.

Samples of the copolymers were denominated  $X/Y$  poly(NBE-*co*-NBD), where  $X$  (80; 60; 40; 20) denotes the initial percentage of NBE and  $Y$  (20; 40; 60; 80) denotes the initial percentage of NBD.

### Characterization

Size exclusion chromatography (SEC) analysis was performed using a Shimadzu Prominence LC system equipped with a LC-20AD pump, a DGU-20A5 degasser, a CBM-20A communication module, a CTO-20A oven, and a RID-10A detector, connected to three PL gel column (5 m MIXED-C: 30 cm,  $\varnothing = 7.5$  mm). The retention time was calibrated with standard monodispersed polystyrene using HPLC-grade  $\text{CHCl}_3$  as eluent. Usually, 50 mg of polymer were dissolved in 10 mL  $\text{CHCl}_3$ , filtered, and injected (20  $\mu\text{L}$ ). PDI (polydispersity index) is  $M_w/M_n$ .

The gel content was analysed via Soxhlet extraction. A 2–3 g sample was placed into a cellulose thimble that was subsequently placed in a Soxhlet extractor equipped with a 250-mL round-bottom flask containing toluene. A condenser was placed on top of the extractor, and the sample was refluxed for 24 h. After refluxing, the insoluble portion was dried for 24 h in a vacuum oven and weighed.

Swelling tests in toluene were performed to evaluate the occurrence of cross-link in the isolated polymers from ROMP. The samples were weighed to determine the

initial weights ( $w_{\text{initial}}$ ) and soaked in toluene at 25 °C. After 24 h the final weights ( $w_{\text{final}}$ ) of samples were obtained. The swelling degree percentage (SD %) was calculated using the Eq. (1). The swollen polymers were dried to weigh the  $w_{\text{dry}}$  to estimate the cross-link degree percentage (CD %) using the Eq. (2):

$$\text{SD \%} = [(w_{\text{final}} - w_{\text{initial}})/w_{\text{initial}}] \times 100, \quad (1)$$

$$\text{CD \%} = (w_{\text{dry}}/w_{\text{swelled}}) \times 100. \quad (2)$$

Nuclear magnetic resonance (NMR) analysis was performed using an Agilent model 500/54 Premium Shielded 500 MHz. For  $^{13}\text{C}\{^1\text{H}\}$  without NOE NMR analyses of the copolymers, 150 mg of polymer was dissolved in 10 mL of  $\text{CHCl}_3$ , and an aliquot (300  $\mu\text{L}$ ) was added to the NMR tube with  $\text{CDCl}_3$  (number of scans = 3200, acquisition time = 14 h, pulse angle = 90°, and relaxation delay = 15 s). For the COSY NMR experiment, the complex was added to a fresh monomer solution (norbornadiene) in  $\text{CDCl}_3$  with molar ratio of [complex]/[NBD] = 2 (acquisition time = 42 min, 8 scans per  $t_1$  increment, and 256  $t_1$  increments).

Scanning electron microscopy (SEM) was performed using a LEO 440 ZEISS/LAICA (Cambridge, England) with an EDX OXFORD system (model 7060). The samples were coated with 10 nm of gold utilizing a BAL-TEC MED020 coating system (BAL-TEC, Liechtenstein).

Differential scanning calorimetry (DSC) analysis was performed using a TA Instrument Q2000 thermal analyzer. The samples were heated from  $-50$  °C up to 200 °C at a heating rate of 10 °C  $\text{min}^{-1}$  to erase their thermal history, equilibrated at  $-50$  °C, and then heated to 200 °C with a heating rate of 10 °C  $\text{min}^{-1}$ . The  $T_g$  values determined from the second scans.

Thermogravimetric analysis (TGA) was performed using a thermal analyser (TA Instrument Q50). The samples were heated from room temperature to 700 °C at a heating rate of 20 °C  $\text{min}^{-1}$  under flow of air at 60  $\text{mL min}^{-1}$ .

Dynamical mechanical analysis (DMA) was performed using a TA Instruments DMA Q800 dynamic mechanical analyser with a film tension mode of 1 Hz. Rectangular specimens was used for the analysis. Samples were cooled and held isothermally for 2 min at  $-50$  °C before the temperature was increased up to 70 °C at a rate of 3 °C  $\text{min}^{-1}$ .

## Results and discussion

### ROMP of NBD with complex 1

Reaction time, solvent volume, and atmosphere type were selected as parameters to evaluate the activity of **1** in ROMP of NBD at 25 °C (Table 1).

Under argon atmosphere, quantitative yield was obtained with 2 mL of solvent for 5 min, decreasing in yield when the reactions were performed with more solvent (Table 1; entries 1–4). With 4–8 mL of solvent, methanol was added to stop the

**Table 1** Dependence of the polyNBD yield obtained with **1** on the reaction time, CHCl<sub>3</sub> volume, and atmosphere type at 25 °C

Entry	Time (min)	Volume (mL)	% Yield (in argon)	% Yield (in air)	Yield <sub>argon</sub> /yield <sub>air</sub> ratio		
					With <b>1</b>	With <b>2</b> <sup>a</sup>	With <b>3</b> <sup>b</sup>
1	5	2	100	74	1.4	1.2	1.5
2	5	4	54	26	2.1	2.7	2.8
3	5	6	22	11	2.0	2.1	3.2
4	5	8	11	*	*	*	8.2
5	30	2	100	100	1.0	0.9	1.3
6	30	4	100	51	2.0	1.3	1.7
7	30	6	100	20	5.0	4.0	3.0
8	30	8	100	*	*	*	4.3
9	60	2	100	92	1.1	1.0	1.2
10	60	4	100	18	5.6	1.1	1.8
11	60	6	100	*	*	1.8	2.7
12	60	8	100	*	*	*	6.7
13	120	2	100	94	1.1	1.0	1.0
14	120	4	100	27	3.7	1.0	1.5
15	120	6	100	*	*	1.9	2.4
16	120	8	100	*	*	2.8	6.7

<sup>a</sup>Data from ref. [21]<sup>b</sup>Data from ref. [24]

\* Less than 5% yield under air or no occurrence of polymer in significant yield to be isolated

reactions and turbid solutions were observed. This turbidity can be associated with the interruption of the propagating chains, and polymers with low molecular weights remained in solution. Probably, more chains or cross-linked chains were initiated at large volumes. In addition, ROMP reactions are generally disfavoured thermodynamically at low reagent concentration (large volume) [16, 20].

When the reactions were conducted for more than 30 min, quantitative yields were obtained regardless of the solvent volume (Table 1; entries 5–16). Thus, extended reaction time favoured the occurrence of full conversion of NBD into polymer at large volumes, when small chains were initiated in the first minutes of reaction and propagated over time.

In all the cases, the resulting polymers were insoluble in CHCl<sub>3</sub> and THF—in agreement with an expected cross-linked network—and the molecular weights were not determined.

Quantitative yields of polyNBD under argon atmosphere were obtained with **3** for 5 min at 25 °C regardless of solvent volume [17]. With complex **2**, quantitative yields were only obtained for 60 min at 40 °C [22]. This suggests the following complex reactivity series for ROMP of NBD: **1** ~ **3** > **2**.

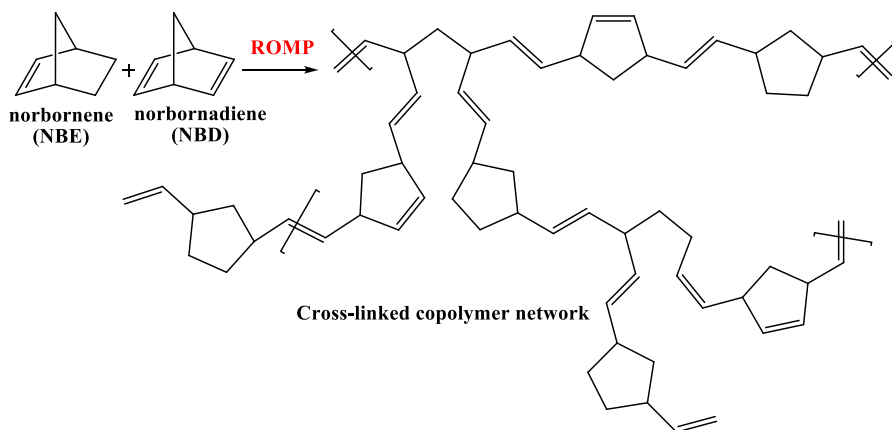
Previous studies have shown quantitative yields of polyNBE with complex **1** only when the reaction occurred for 120 min in 2–8 mL of solvent under argon atmosphere at 25 °C [29], which suggests better reactivity of **1** with NBD compared with that with NBE, as occurred with complex **3** [17].

In air, quantitative or semi-quantitative yields were obtained with 2 mL of solvent with reaction time longer than 30 min (Table 1; entries 5, 9 and 13). Lower yields were obtained when solvent volume was increased for any reaction time. As the Ru(II) complex forms the metal carbene in an induction period, before reaction with the first monomer unit (initiation step), oxidation of the active species by O<sub>2</sub> from air dissolved in solution explains the low yields obtained at larger volumes with increasing time [17, 29]. Therefore, the Ru complexes in the initiated chains probably undergo oxidations by the molecular oxygen dissolved in the solvent at large volumes for long periods, and the propagation step fails. In contrast, in 2 mL of solvent, the propagation step tends to occur either under argon atmosphere or in air. It is worth noting that the yield<sub>argon</sub>/yield<sub>air</sub> ratios are close to 1.0 with 2 mL CHCl<sub>3</sub> for reaction time longer than 30 min (Table 1; entries 5, 9, and 13). From early studies, complex **3** tends to provide similar behaviour [17]. Complex **2** also shows good yields with 4 mL of solvent [17]. From these data, it is possible to conclude that the complexes **1**, **2**, and **3** showed good activity in ROMP of NBD in non-degassed solution with 2 mL CHCl<sub>3</sub>.

### ROMP of NBD in the presence of NBE with complex **1**

Different loadings of NBD were added to NBE solutions to obtain copolymers via ROMP with complex **1** (Scheme 3).

Under argon atmosphere, with 80% of NBD in the starting composition, the high quantity of this monomer probably favours the propagation of polyNBD blocks, as already observed in the aforementioned homopolymerization studies with NBD (Table 2; entry 1). The yield decreased when the NBD amount was reduced from 80



**Scheme 3** Illustration of possible cross-linked copolymer obtained from ROMP of NBD in the presence NBE



**Table 2** Obtained yield values of polymeric materials obtained from ROMP of NBD in the presence of NBE with **1**, in 2 mL CHCl<sub>3</sub> at 25 °C for 120 min

Entry	%NBE/%NBD	Yield % (under argon)	Yield % (under air)	Yield <sub>argon</sub> /yield <sub>air</sub>
1	20/80	100	71	1.4
2	40/60	66	69	0.96
3	60/40	78	71	1.1
4	80/20	83	72	1.2

to 60% (Table 2; entry 2). Perhaps, the reactivity rate favoured the production of homopolymers with low cross-linking: the {Ru-polyNBD} moiety reacting better with NBD than with NBE and the {Ru-polyNBE} moiety reacting better with NBE than with NBD. If the active Ru species favours the reaction with NBD, the growing chain slows down because of the low amount of this monomer. In contrast, propagation with NBD is feasible in the presence of large amounts of this monomer. As a consequence, with low amounts of NBD, occurrence of double coordination can affect ROMP; the yield decreases because NBD is modifying the reaction pathway [27]. There is competition between monomer consumption and double coordination with the presence of up to 60% of NBD.

In air, the resulting polymer yields were ca. 70% for any NBE/NBD starting composition, resulting in yield<sub>argon</sub>/yield<sub>air</sub> ratios close to 1 for 20–60% of NBD (Table 2).

In this type of polymerization reactions, the catalytic performance of complexes **2** and **3** was similar [17]. With complex **3**, the yield increased when the NBD percentage increased. However, considering that polymerizations with complexes **2** and **3** were conducted at 40 °C [27], it can be suggested that **1** shows better catalytic activity because the experiments were conducted at 25 °C.

The sample from the 20/80 NBE/NBD composition was only partly soluble in CHCl<sub>3</sub> probably because high cross-linking degree. The other samples were soluble, which can be associated with the presence of linear blocks in the chains. The <sup>13</sup>C{<sup>1</sup>H} without NOE NMR spectrum in CDCl<sub>3</sub> of the soluble part from the 80/20 sample showed peaks that can be assigned to polymer with NBE and NBD [33, 34]. It was not possible to make a safe interpretation of the reactivity ratio and the *cis-trans* conformation because of the poor spectrum resolutions. Molecular weights of the soluble parts were in the order of magnitude of 10<sup>4</sup> g mol<sup>-1</sup>. The PDI average values were 2.4 from samples obtained under atmosphere argon and 2.8 from samples obtained in air. As expected, this indicates the presence of short chains in the extracted material.

Swelling tests in toluene were performed to evaluate the occurrence of cross-link in the isolated polymers with NBD (Table 3) [15, 35], considering that ROMP of the second double bond in NBD forms a network that can hold solvent molecules (Scheme 3). As expected, all the isolated polyNBE dissolved in toluene, considering that they form linear chains (Scheme 2).

Swelling was observed in polyNBD and polymers from the starting compositions with 80% NBD obtained with **1** and **3** (Table 3; entry 1 and 2), suggesting that

**Table 3** Swelling degree percentage (SD %) in toluene and the cross-link degree percentage (CD %) of polymers obtained with the Ru complexes in 2 mL of  $\text{CHCl}_3$ , at 25 °C for 120 min under air

Entry	Starting composition	SD %; CD %		
		With 1	With 2	With 3
1	NBD	100; 80	100; 27	81; 81
2	20/80 NBE/NBD	100; 27	100; 10	100; 17
3	80/20 NBE/NBD	*	*	100; 25

\* Total dissolution

cross-linked polymers were formed. With complex **2**, polyNBD swelled, but they were partially soluble in toluene, which suggests a low cross-linking degree. Polymers containing only 20% of NBD obtained with complexes **1** and **2** did not swell (Table 3; entry 3), most likely because the amount of NBD was not efficient to obtain a cross-linked polymer, whereas the polymer obtained with complex **3** swelled 100%.

The swollen polymers were dried to estimate the cross-linking degree percentage (CD %), where the remaining weight can be associated with the weight of the cross-linked polymer [36]. The results show polyNBD samples obtained with **1** and **3** with 80% of cross-linking (Table 3; entry 1). The polymers obtained from the starting compositions with 20/80 NBE/NBD swelled, indicating some degree of cross-link, but it was less than 1/3 (Table 3; entry 2). As previously deduced on the reactivity series of the complexes for ROMP of NBD, similar series can be estimated for cross-linking performance: **1** ~ **3** > **2**.

SEM micrographs with 4  $\mu\text{m}$  of resolution of the polymers obtained with complex **1** in air are depicted in Fig. 2, and some correlation with the swelling test can be observed (Table 3). PolyNBE is porous with  $8.55 \pm 0.78 \mu\text{m}$  of average pore size (Fig. 2a), as well the polymer from 20% NBD with  $4.73 \pm 0.17 \mu\text{m}$  of average pore size (Fig. 2b), which dissolved in toluene.

No pores were observed in the material with 20/80 NBE/NBD (Fig. 2c), whereas the polyNBD showed small pores ( $1.50 \pm 0.20 \mu\text{m}$ ; Fig. 2d).

Micrographs from polymers of similar composition obtained with **3** were also analysed (Fig. 3). PolyNBD and polymers obtained from the starting compositions with 20 and 80% NBD did not show pores (Fig. 3b, d). Only polyNBE showed typical porous structures ( $14.32 \pm 0.53$ ; Fig. 3a). These results also support the swelling tests, Table 3, confirming that NBD can form a cross-linking network, but the type of amine as ancillary ligand in the Ru complex influences the resulting polymer.

## Thermal analysis

Thermal analyses were performed to better understand the occurrence of cross-link in the polymers with NBD.

Table 4 summarizes the  $T_g$  values obtained from DSC and DMA measurements of the polymers produced with complex **1**. In addition, similar materials obtained with complexes **2** and **3** were analysed to improve the discussion.

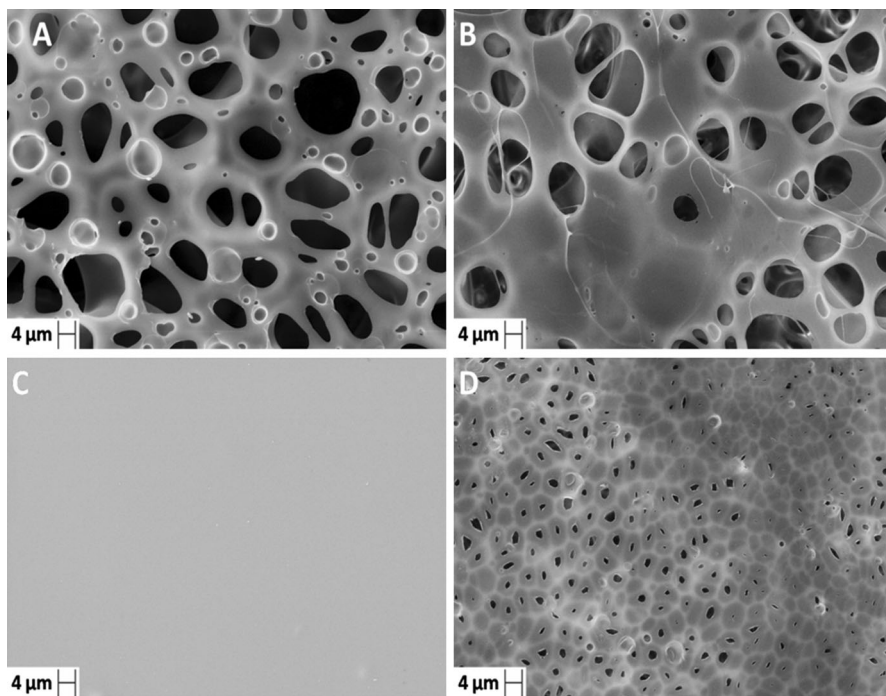


**Fig. 2** SEM micrographs of samples of polyNBE (a), 80/20 poly(NBE-co-NBD) (b), 20/80 poly(NBE-co-NBD) (c), and polyNBD (d) obtained with **1** in air. At 25 °C for 120 min under air

The samples from polyNBE showed  $T_g$  values independent from the starting complex, both by the DSC and DMA techniques (Fig. 4; Table 4). These results are in agreement with a linear chain of polyNBE with structure and character of a thermoplastic with low  $T_g$  [26]. In contrast, the polyNBD samples showed results dependent on the complex used, with  $T_g$  values in the range from 20 to 50 °C (Fig. 4). The polyNBD obtained with **1** presented higher  $T_g$  than the polyNBD obtained with **3**. The results from the polyNBD samples suggest the occurrence of cross-linked lattice, and this depends on the starting complex. In addition, the possible cross-linked lattice from NBD is in contrast with the expectation that NBD is a poor cross-linking agent [36]. In the case of polyNBE samples, the lower values in the curves (around zero degree) are associated with the molecule rotation around the C=C double bond when polyNBE presents high *trans* content [17, 22, 25, 29].

When 80% NBD was in the composition, the DSC curves were flat; many times cross-linked copolymers are not expected to show defined  $T_g$  values. DMA measurements were not performed with polyNBD because of the brittle nature of the obtained materials. This was not the case with the samples from 80/20 NBE/NBD, with  $T_g$  values around 50–57 °C from  $\tan \delta$  curves (Fig. 5; Table 4), and they are close to those observed in the polyNBE samples. This suggests that large polyNBE blocks can be present in the polymer chains. It is interesting to observe that the processes associated with molecule rotation around the C=C double bond

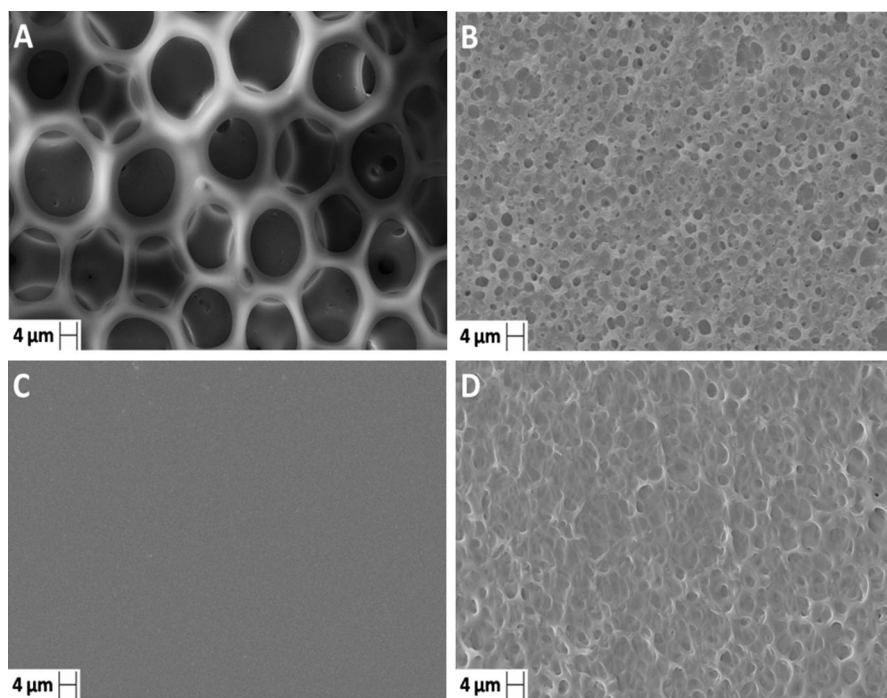


**Fig. 3** SEM micrographs of samples of polyNBE (**a**), 80/20 poly(NBE-co-NBD) (**b**), 20/80 poly(NBE-co-NBD) (**c**), and polyNBD (**d**) obtained with **3** in air. At 25 °C for 120 min under air

**Table 4**  $T_g$  values from second DSC scans and from DMA curves of the polymers

Complex	Starting composition	$T_g$ from DSC (°C)	$T_g$ from DMA (°C)
<b>1</b>	NBE	48.0	~ 50
	NBD	48.3	*
	80/20 NBE/NBD	ND	51.3
<b>2</b>	NBE	47.3	~ 50
	NBD	39.2	*
	80/20 NBE/NBD	ND	50.0
<b>3</b>	NBE	46.6	~ 50
	NBD	22.7	*
	80/20 NBE/NBD	ND	56.5

ND not defined transition

\* Brittle

are in lower values in the curves (around  $-20$  °C) than in the samples of the homopolyNBE.

Figure 6 shows the storage modulus ( $E'$ ) curves as a function of temperature for polyNBE. The variation in the  $E'$  values indicates that the resulting polymers present some distinction depending on the starting complex used in the synthesis.

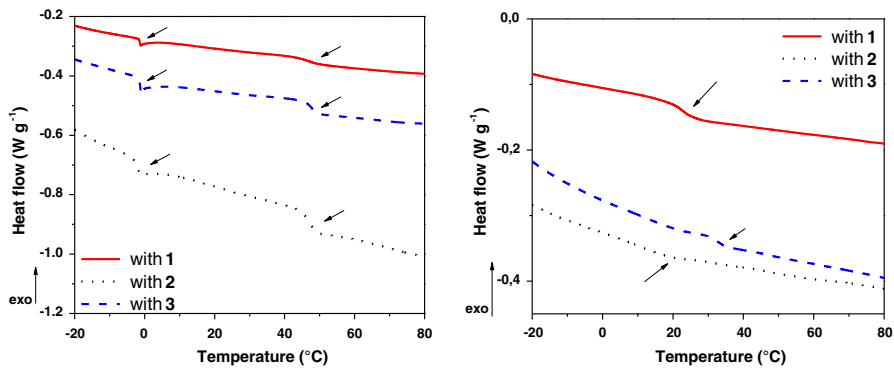


**Fig. 4** Second DSC scans of polyNBE (top) and polyNBD samples

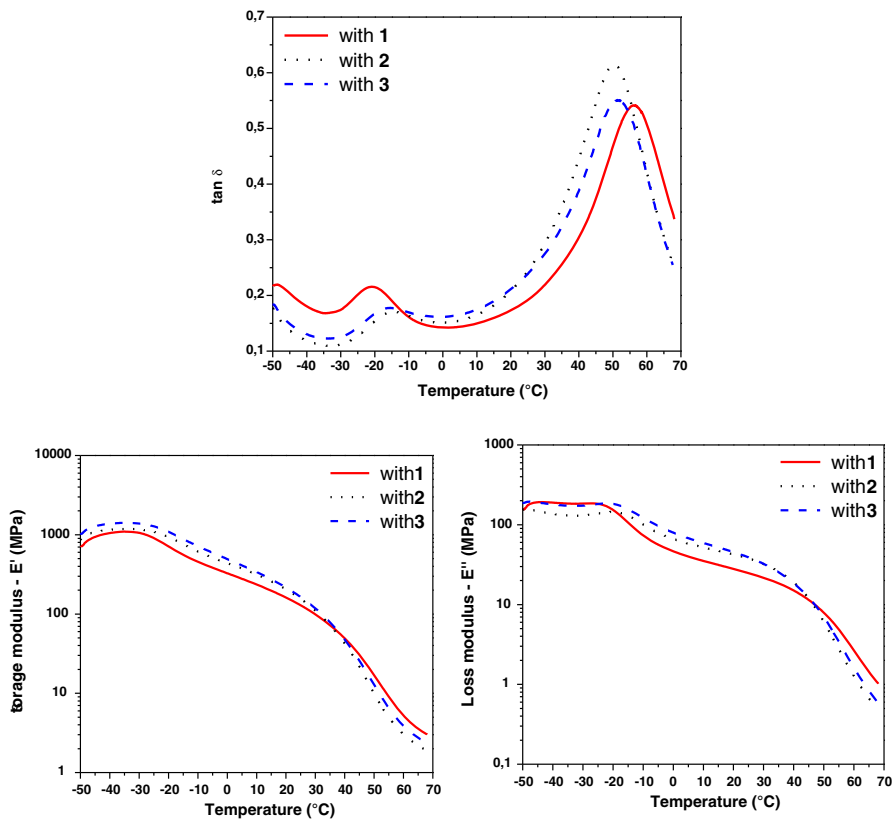


**Fig. 5** DMA curves of 80/20 NBE/NBD films

The measurements indicate that all polyNBEs exist in glassy state at low temperature, in the range of  $-20$  to  $0$  °C. The  $E'$  values slightly decrease when the temperature rises to  $0$  °C, and then two sequential abrupt drops are observed in

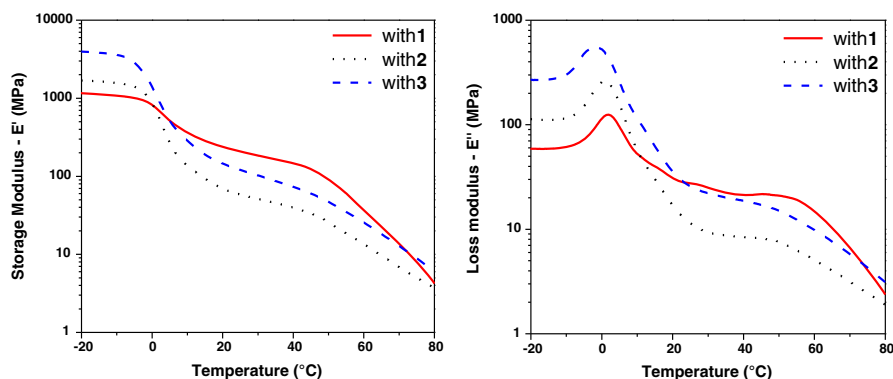


**Fig. 6** DMA curves for films of polyNBE obtained with the complex **1**, **2**, and **3**

the temperature range from 0 to 60 °C in all of the cases. These processes correspond to the primary relaxation ( $\alpha$ ) of the chain segments of polyNBE. The first event is associated with *trans* conformation for NBE units, followed by molecular mobility of the *cis*-NBE units. The polymers reach the rubbery plateau above 80 °C. The higher  $E'$  values from polyNBE obtained with **1** and **2** compared with the value obtained with **3** suggest that the molecular weights of the first are higher than that of the latter, which is in agreement with the early DSC and SEC results, in the order of magnitude of  $10^5 \text{ g mol}^{-1}$  [17, 22, 29]. The  $T_g$  values for polyNBE obtained with **1**, **2**, and **3**, as determined from the maxima in the  $\tan \delta$  curves, are in agreement with the  $T_g$  values observed in the DSC curves (Table 4).

In general, the TGA curves with different complexes for each polymer set with the same monomer starting composition presented the same degradation profile (Fig. 7).

PolyNBEs were stable until 350 °C and presented two degradation steps (Fig. 7a). The small weight loss before 350 °C can be attributed to the decomposition of small polymer chains. The main degradation step (350–500 °C) can be associated with decomposition of the polymer backbone. The final loss at ca. 500 °C is associated with oxidation of the carbon residues.

The curves of poly(NBE-co-NBD) with 20 and 80% of NBD in the starting composition show drops in weight loss up to 400 °C, characterized by decomposition of the cross-linked lattice, followed by decomposition of the polymer backbone (Fig. 7b, c). The TGA curves for polyNBDs showed a similar profile, where three degradation steps were also observed (Fig. 7d). The first loss (up to 425 °C) is associated with decomposition of the cross-linked lattice. The second loss (up to 500 °C) and final loss are associated with decomposition of the polymer backbone and oxidation of the carbon residue, respectively, as occurred with polyNBE. It is worth noting that weight loss differs in the samples with NBD from polyNBE; the curves for polyNBE are similar. T10 occurs at ca. 400 °C in the case of polyNBE, but at ca. 100 °C in the case of NBD. T50 occurs at ca. 450 °C in all the cases. This feature can be associated with the different reactivity of complexes with NBD.

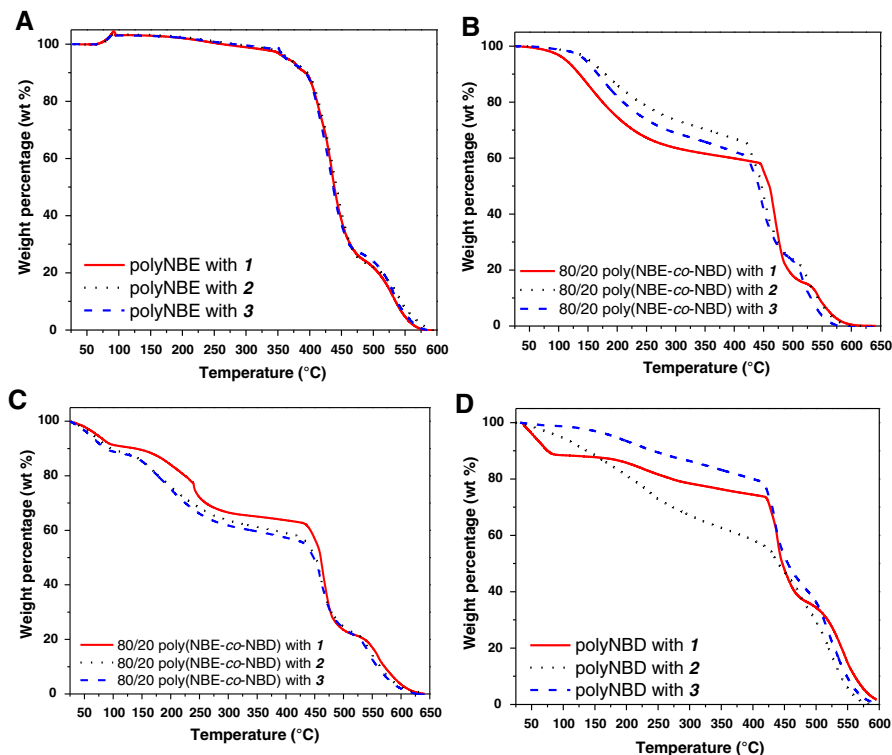


**Fig. 7** TGA curves of polyNBE (a), 80/20 poly(NBE-co-NBD) (b), 20/80 poly(NBE-co-NBD) (c), and polyNBD (d)

## Conclusion

The  $[\text{RuCl}_2(\text{PPh}_3)_2(\text{pyrrolidine})]$  complex (**1**) exhibited activity for ROMP of NBD either under argon atmosphere or in air at 25 °C. Under argon atmosphere, this complex was more active with NBD than with NBE for short times regardless of the solvent volume studied. In air, good yields were only obtained in 2 mL of  $\text{CHCl}_3$  probably due to oxidation of the active species at large volumes, which was less pronounced with NBE. The  $\text{yield}_{\text{argon}}/\text{yield}_{\text{air}}$  ratios from the copolymerization studies were close to 1.0 for all NBE/NBD compositions. Considering that ROMP reactions between NBD and NBE with complexes with piperidine and perhydroazepine as amines were conducted at 40 °C, it can be suggested that complex **1** shows better catalytic activity, considering that the experiments were conducted at 25 °C. The swelling tests showed that complexes **1** and **3** were able to form cross-link in the presence of NBE. The micrographs from polyNBE samples presented pores, and in polymers with NBD, the pores tended to decrease in size. DSC scans showed defined  $T_g$  values that characterize the polyNBE as thermoplastics with high *trans* content. The DMA experiments are in agreement with the  $T_g$  values from the DSC measurements, and the higher the  $E'$  value from polyNBE obtained with **2** and

**3** compared with that obtained with **1** suggests that the molecular weights of the first are higher than that of the latter, which is in agreement with the SEC results. PolyNBD and samples from 20/80 NBE/NBD films were too brittle to perform DMA measurements, but the  $T_g$  values of polyNBD from DSC scans were similar to those reported in the literature (35 °C). The thermal characteristics of polyNBD and copolymer were influenced by the complex utilized due to the efficiency of each to form cross-linking. Therefore, the complexes were active to open the second double bond of NBD and to shift the thermoplastic characteristic of polyNBE in the presence of NBD.

**Acknowledgements** The authors are indebted to FAPESP (Process numbers 2011/12571-7 and 2012/23948-7), CAPES and CNPq for the financial support. The DMA, DSC and TGA analyses were conducted in the Polymer Composites Research Group of the Department of Materials Science and Engineering, Iowa State University, during L. R. Fonseca's PhD internship, and we are grateful.

## References

1. Mol JC (2004) Industrial applications of olefin metathesis. *J Mol Catal A Chem* 213(1):39–45
2. Ding R, Xia Y, Mauldin TC, Kessler MR (2014) Biorenewable ROMP-based thermosetting copolymers from functionalized castor oil derivative with various cross-linking agents. *Polymer* 55(22):5718–5726
3. Spring AM, Maeda D, Ozawa M, Odoi K, Qiu F, Yamamoto K, Yokoyama S (2015) An analysis of the structural, thermal and optical characteristics as well as the electrical resistivity of tert-butylidiphenylsilyl substituted poly(norbornene-dicarboximide)s. *Polymer* 56:189–198
4. Bochkarev LN, Rozhkov AV, Ilichev VA, Abakumov GA, Bochkarev MN (2014) Green-light emitting norbornene based terbium-containing copolymers. Synthesis, photo- and electroluminescent properties. *Synth Met* 190:86–91
5. Leitgeb A, Wappel J, Slugovc C (2010) The ROMP toolbox upgraded. *Polymer* 51(14):2927–2946
6. Bielawski CW, Grubbs RH (2007) Living ring-opening metathesis polymerization. *Prog Polym Sci* 32(1):1–29
7. Carvalho VP Jr, Ferraz CP, Silva Sá JL, Lima-Neto BS (2012) Romp como um método versátil para a obtenção de materiais poliméricos diferenciados. *Quim Nova* 35(4):791–801
8. Hollauf M, Trimmel G, Knall AC (2015) Dye-functionalized polymers via ring opening metathesis polymerization: principal routes and applications. *Monatsh Chem* 146(7):1063–1080
9. Yao PS, Cao QY, Peng RP, Liu JH (2015) Quinoline-functionalized norbornene for fluorescence recognition of metal ions. *J Photochem Photobiol A Chem* 305:11–18
10. Hu F, Zheng Y, Fang Y, Ren X, Liu X (2014) Preparation and properties of cyclopentadiene-containing monomer modified polydicyclopentadiene. *Polymer* 55(12):2809–2816
11. Deraedt C, d'Halluin M, Astruc D (2013) Metathesis reactions: recent trends and challenges. *Eur J Inorg Chem* 2013(28):4881–4908
12. Xia Y, Larock RC (2010) Castor oil-based thermosets with varied crosslink densities prepared by ring-opening metathesis polymerization (ROMP). *Polymer* 51(12):2508–2514
13. Yoon K-H, Kim KO, Schaefer M, Yoon DY (2012) Synthesis and characterization of hydrogenated poly(norbornene endo-dicarboximide)s prepared by ring opening metathesis polymerization. *Polymer* 53(11):2290–2297
14. Benson SW, Cruickshank FR, Golden DM, Haugen GR, O'Neal HE, Rodgers AS, Shaw R, Walsh R (1969) Additivity rules for the estimation of thermochemical properties. *Chem Rev* 69(3):279–324
15. Sheng X, Lee JK, Kessler MR (2009) Influence of cross-link density on the properties of ROMP thermosets. *Polymer* 50(5):1264–1269
16. Ivin KJ, Mol JC (1997) Olefin metathesis and metathesis polymerization. Academic Press, San Diego
17. Silva Sá JL, Vieira LH, Nascimento ESP, Lima-Neto BS (2010) The influence of perhydroazepine and piperidine as further ancillary ligands on Ru-PPh<sub>3</sub>-based catalysts for ROMP of norbornene and norbornadiene. *Appl Catal A Gen* 374(1–2):194–200



18. Chauvin Y (2006) Olefin metathesis: the early days (nobel lecture). *Angew Chem Int Ed* 45(23):3740–3747
19. Grubbs RH (2004) Olefin metathesis. *Tetrahedron* 60(34):7117–7140
20. Fürstner A (2000) Olefin metathesis and beyond. *Angew Chem Int Ed* 39(17):3012–3043
21. Leingruber S, Trimmel G (2015) Olefin metathesis meets rubber chemistry and technology. *Monatsh Chem* 146(7):1081–1097
22. Matos JME, Lima-Neto BS (2004) Piperidine as ancillary ligand in the novel  $[\text{RuCl}_2(\text{PPh}_3)_2(\text{piperidine})]$  complex for metathesis polymerization of norbornene and norbornadiene. *J Mol Catal A Chem* 222(1–2):81–85
23. Matos JME, Lima-Neto BS (2006) Acyclic amines as ancillary ligands in Ru-based catalysts for ring-opening metathesis polymerization: probing the electronic and steric aspects of cyclic and acyclic amines. *J Mol Catal A Chem* 259(1–2):286–291
24. Silva Sá JL, Lima-Neto BS (2009) Ability of Ru complexes for ROMP tuned through a combination of phosphines and amines. *J Mol Catal A Chem* 304(1–2):187–190
25. Carvalho VP Jr, Ferraz CP, Lima-Neto BS (2010) Electronic synergism in  $[\text{RuCl}_2(\text{PPh}_3)_2(\text{amine})]$  complexes differing the reactivity for ROMP of norbornene and norbornadiene. *J Mol Catal A Chem* 333(1–2):46–53
26. Carvalho VP Jr, Ferraz CP, Lima-Neto BS (2012) Tailored norbornene-based copolymer with systematic variation of norbornadiene as a crosslinker obtained via ROMP with alternative amine Ru catalysts. *Eur Polym J* 48(2):341–349
27. Silva Sá JL, Nascimento ESP, Fonseca LR, Lima-Neto BS (2013) Ring opening metathesis copolymerization of norbornene with norbornadiene from solutions with different mole fractions of the comonomers catalyzed by Ru–amine complexes. *J Appl Polym Sci* 127(5):3578–3585
28. Chaves HK, Ferraz CP, Carvalho VP Jr, Lima-Neto BS (2014) Tuning the activity of alternative Ru-based initiators for ring-opening metathesis polymerization of norbornene and norbornadiene by the substituent in 4-CH<sub>2</sub>R-piperidine. *J Mol Catal A Chem* 385:46–53
29. Fonseca LR, Nascimento ESP, Silva Sa JL, Lima-Neto BS (2015) The ring size of cyclic amines as a relevant feature in the activity of Ru-based complexes for ROMP. *New J Chem* 39(5):4063–4069
30. Fernandes RJ, Silva TB, Lima-Neto BS, Haiduke RLA (2015) Structural and kinetic insights into the mechanism for ring opening metathesis polymerization of norbornene with  $[\text{RuCl}_2(\text{PPh}_3)_2(\text{piperidine})]$  as initiator complex. *J Mol Catal A Chem* 410:58–65
31. Guidone S, Songis O, Nagra F, Cazin CSJ (2015) Conducting olefin metathesis reactions in air: breaking the paradigm. *ACS Catal* 5(5):2697–2701
32. Fernandes RJ, Silva TB, Lima-Neto BS, Haiduke RLA (2015) Structural and kinetic insights into the mechanism for ring opening metathesis polymerization of norbornene with  $[\text{RuCl}_2(\text{PPh}_3)_2(\text{piperidine})]$  as initiator complex. *J Mol Catal A Chem* 410(15):58–65
33. Bell B, Hamilton JG, Mackey OND, Rooney JJ (1992) Microstructure of ring-opened polymers and copolymers of norbornadiene. *J Mol Catal* 77(1):61–73
34. Czeluśniak I, Szymańska-Buzar T (2002) Ring-opening metathesis polymerization of norbornene and norbornadiene by tungsten(II) and molybdenum(II) complexes. *J Mol Catal A Chem* 190(1–2):131–143
35. Henna P, Larock RC (2009) Novel thermosets obtained by the ring-opening metathesis polymerization of a functionalized vegetable oil and dicyclopentadiene. *J Appl Polym Sci* 112(3):1788–1797
36. Sheng X, Kessler MR, Lee JK (2007) The influence of cross-linking agents on ring-opening metathesis polymerized thermosets. *J Therm Anal Calorim* 89(2):459–464